Korean J. Chem. Eng., 36(12), 2125-2132 (2019)
DOI: 10.1007/s11814-019-0395-7

pISSN: 0256-1115
eISSN: 1975-7220

Enhanced proton conductivity of sulfonated poly(ether ether ketone) membranes at elevated temperature by incorporating (3-aminopropyl)triethoxysilane-grafted graphene oxide

Shuguo Qu†, Chenchen Zhang, Minhui Li, Yan Zhang, Lunbo Chen, Yushuai Yang, Bo Kang, Yiwei Wang, Jihai Duan, and Weiwen Wang

College of Chemical Engineering, Qingdao University of Science & Technology, Qingdao, Shandong 266042, China
(*Received 27 June 2019 • accepted 24 September 2019*)

Abstract−Making inexpensive proton exchange membrane with high proton conductivity for the proton exchange membrane fuel cell (PEMFC) is still a challenging problem. Graphene oxide (GO) nanoparticles grafted with (3-aminopropyl) triethoxy silane (APTES) were prepared and then incorporated into sulfonated poly(ether ether ketone) (SPEEK) matrix by solution casting to make the composite proton exchange membrane. The obtained nanoparticles and composite membranes were characterized by XRD, FT-IR, Raman, TGA, SEM, and UTM. GO treated with the silane coupling agent improved the dispersion stability and compatibility of GO in SPEEK, which decreased the agglomeration of GO nanoparticles in the SPEEK membrane. The prepared nanocomposite membranes exhibited better water retention properties and proton conductivity. The proton conductivity of the SPEEK membrane with 2 wt% amine functionalized GO (AGO) reached 11.32 mS/cm at 120 °C, which was 2.45-times higher than that of the pristine SPEEK membrane. The reason was that AGO nanoparticles disperse uniformly in the SPEEK membranes, which provides new channels for proton transfer. The potential application of this composite membrane in the PEMFC was indicated.

Keywords: SPEEK, Amine Functionalized Graphene Oxide, Proton Exchange Membrane, Proton Conductivity

INTRODUCTION

As a new energy environmental protection device, fuel cells can generate electrical energy through electrochemical reaction [1]. Among various fuel cells, the proton exchange membrane fuel cell (PEMFC) has been extensively studied for its high conversion efficiency, wide source of hydrogen, fast start-up, and zero emission [2]. The proton exchange membrane (PEM), which transfers proton and blocks fuel penetration, is a key component of the PEMFC, and its properties directly affect the performance and the life of the PEMFC. Currently, the most used PEM is Nafion® membrane [3-7], which has better mechanical properties and proton conductivity, but there are two obvious disadvantages [8]: first, the production process is difficult and costly; secondly, the proton conductivity is poor at high temperature (>80 °C), and methanol permeability is high. To resolve these challenging problems, a PEM which could replace Nafion® has been studied for decades. The most popular substitute materials are sulfonated aromatic polymers, including sulfonated polyimides (SPI) [9-11], sulfonated poly(arylene ether sulfones) (SPAES) [12], sulfonated polyethersulfones (SPES) [13-16], and sulfonated poly(ether ether ketone) (SPEEK) [17-25].

Compared with Nafion®, SPEEK has certain proton conductivity, better thermal stability, distinguished methanol barrier properties and is relatively inexpensive. The degree of sulfonation (DS) of SPEEK affects its performance. High DS results in high proton conductivity [22]. However, the decomposition of the sulfonic acid group leads to the membrane swelling increasing, and the stability of the composite membrane decreases during long-term use [23-25]. It has been found that the performance of the SPEEK membrane could be effectively enhanced by introducing various inorganic nanofillers, such as silica (SiO_2) [26,27], sulfonated silica ($SSiO_2$) [28], Fe_2TiO_5 (IT) [29], tin oxide [30], montmorillonite [31], $Ba_{0.9}Sr_{0.1}TiO_3$ (BST) [32], sulfonated core-shell TiO_2 [33], and graphene oxide [34-41]. Therefore, the addition of functionalization nano-fillers is convenient for constructing proton transfer channels in the PEM [19], and it reduces the swelling degree of the SPEEK membrane with higher DS.

In recent years, graphene oxide (GO) has intrigued many researchers in academia and industry thanks to its large surface area, excellent thermal, and promoting proton conduction [42-47]. GO sheets are two-dimensional nanomaterials which have a variety of functional group [34,35]. Mohammad et al. [45] synthesized magnetite-coated molybdenum disulfide and reduced graphene oxide (Fe_3O_4 @MoS_2/RGO) hybrid three-component nanoelectrocatalyst to effectively replace platinum catalyst in DMFC, and showed better result. The high specific surface area provides more geological sub-transport channels and numerous functional groups allowing GO to retain more moisture. As an inorganic filler, GO can effectively compromise the problem between proton conductivity and swelling of the polymer membranes [46-49]. It also endows the nanocomposite membrane with enhanced strength [50]. It was found that the valid incorporation and better dispersion of GO within the poly-

†To whom correspondence should be addressed.
E-mail: shuguoqu@163.com

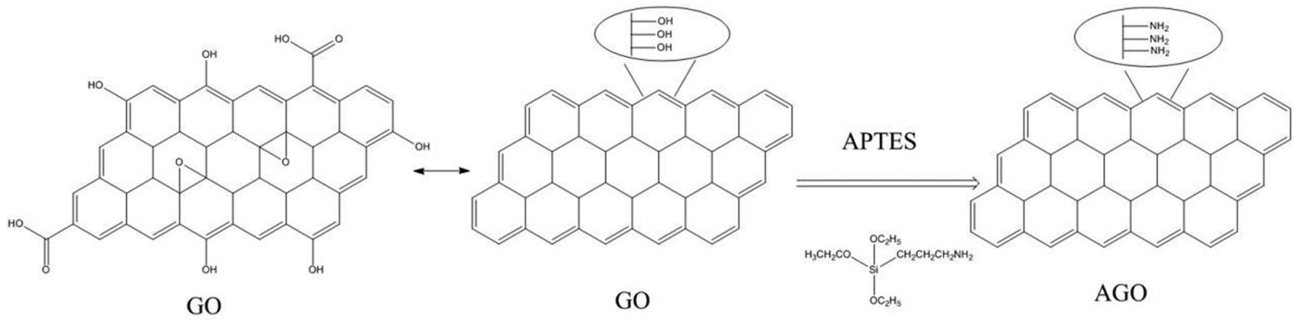

Fig. 1. Schematic of synthesis of AGO nanoparticles.

mer membranes is the pivotal challenge to achieve better performance of the PEM [39]. Thus, how to relieve or eliminate GO nanoparticles aggregation effect during the preparation of the PEM has aroused many researchers' attention. Polydopamine modified GO was prepared and then added in the SPEEK membrane to prepare a nanocomposite membrane [51]. By adjusting the nanophase separation structure and chain mobility of the composite membrane, it exhibited enhanced chemical stability and improved proton conductivity at 120 °C and 100% relative humidity (RH). Zarrin et al. [4] prepared 3-mercaptopropyltrimethoxysilane modified GO, which was then added to the Nafion® polymer membrane. The proton conductivity of the prepared composite membrane was higher than that of pure Nafion® membrane at 120 °C, RH=25%. Sulfonic acid functionalized GO (SPB-FGO) was added into the SPES polymer membrane [12]. Due to the uniform distribution of SPB-FGO in the SPES membranes, broad and continuous proton conduction pathway was formed, both proton conductivity and chemical stability were improved. Salanizadeh et al. [18,19] added amine-functionalized iron titanate (AIT) and amine-functionalized titanium dioxide (AFT) into the SPEEK membrane. The made composite membranes all displayed improved performance including chemical stability, water retention, and electrical conductivity. Chiong et al. [52] added 3-aminopropyltriethoxysilane (APTES)-GO to polyvinylidene fluoride (PVDF), and found that nanocomposite coatings exhibited excellent corrosion resistance and good adhesion in corrosive environments. Feng et al. [53] added APTES functionalized GO to sulfonated poly(arylene ether nitrile) (SPEN), and interfacial ionic nanochannels were established to provide fast proton transfer channel. Rehman et al. [54] prepared of SPI polymer grafted by sulfonated imidized GO (SIGO), resulting in the separation of hydrophobic-hydrophilic phase, and the proton conductivity of membrane reached 0.11 S/cm at room temperature. However, the incorporation of GO nanoparticles modified by APTES into the matrix of SPEEK used for high temperature PEMFC has not been reported.

We used APTES as a silane coupling agent, which was grafted onto the surface of GO. Then, the amine functionalized GO (AGO) was introduced into the matrix of SPEEK with the method of solution casting. The obtained nanoparticles and composite membranes were characterized by XRD, FT-IR, Raman, TGA, SEM, and UTM. Comparisons including water uptake, membrane swelling, mechanical property, thermal property, proton conductivity between the SPEEK/AGO membranes and the pristine SPEEK membranes were made in this paper.

EXPERIMENTAL

1. Materials

PEEK (American Victrex Corporation, 450PF), concentrated sulfuric acid (98%), GO (Chinese Academy of Sciences Chengdu Organic Chemistry Co., Ltd.), 3-aminopropyltriethoxysilane (APTES) (Aladdin Reagent (Shanghai) Co., Ltd.), N,N-dimethylformamide (DMF) (National Pharmaceutical Group Chemical Reagent Co., Ltd.).

2. Amine Functionalized GO and Sulfonation of PEEK

AGO was prepared according to literature [13]. GO was sonicated in ethanol to obtain a uniform GO dispersion, then 5 mL of APTES was precipitated in the above reaction system and under ultrasound for 1 h. After that, the reaction product was stirred at 70 °C for 6 h. Then, the mixture was washed several times with ethanol and deionized water to remove unreacted APTES and then filtered. Finally, the obtained product was dried under vacuum at 60 °C for 12 h to obtain the AGO black powder. The amine-functionalization reaction of GO nanoparticles is shown in Fig. 1.

SPEEK was prepared according to the procedure reported by our group [55]. First, the PEEK was dried at 120 °C under vacuum for 24 h. Then, 2.5 g of PEEK was added to 50 mL H_2SO_4 and vigorously stirred at 70 °C about 2.5 h. After that, the product was added into an ice-water bath under mechanical agitation. The precipitate was washed with de-ionized water till neutralized and finally dried under vacuum oven at 80 °C for day. The DS of the SPEEK in this paper was found to be 76% by titration method [55].

3. Synthesis of SPEEK/AGO Composite Membranes

The SPEEK/AGO nanocomposite membranes were prepared according to the procedure in literature reported by our group with the method of solution casting [55]. First, SPEEK was dissolved in DMF at room temperature. Different weight percentages of AGO were added to DMF under ultrasonic condition for 1 h. Then SPEEK/DMF solution was added to the AGO/DMF mixture at 70 °C under stirring for about 3 h. The homogeneous suspension was directly cast in a petri dish and dried in a vacuum at 70 °C for overnight. The prepared membranes were expressed as SPEEK/X-AGO, the X denotes the ratio of AGO weight to SPEEK and AGO weight (0%, 1%, 2%, 3%, 4%, 5%).

4. Characterizations

4-1. FT-IR

The functional groups of GO and AGO were analyzed using Fourier transform infrared spectrometer (FT-IR, Thermo Scientific Nico-

let iS10). The scanning wavelength ranged between 4,000 cm^{-1} and 400 cm^{-1}.

4-2. XRD

The crystalline behavior of the GO and AGO nanoparticles was measured by 2500 (Rigaku, Japan) X-ray diffractometer (XRD). The scanning ranged between 5° and 40° using Cu Kα radiation.

4-3. Raman

The microstructures of the GO and AGO nanoparticles were analyzed using a (LabRRM HR Evolution) Raman spectrometer. The scanning ranged between 500 cm^{-1} and 2,500 cm^{-1}.

4-4. SEM

The morphologies of GO, AGO and SPEEK/AGO composite membrane were characterized by JSM-7800F (JEOS Ltd, Japan) scanning electron microscope. The surface morphology, surface roughness and cross-sectional morphology were observed.

4-5. TGA

A TG 209F1 TGA analyzer (Bochum, Germany) type thermogravimetric analyzer was used to measure the thermal stability of the composite membrane under a nitrogen atmosphere. The temperature ranged from 30 °C to 800 °C with the heating rate 10 °C/min.

4-6. Mechanical Properties

Mechanical properties of the SPEEK/AGO membranes with a size of 50 mm×10 mm were tested using a MODEL/UTM2502 universal material tester at an operating speed of 5 mm/min.

4-7. Water Uptake and Membrane Swelling

First, three groups of SPEEK/AGO membranes with 1 cm×1 cm were dried at 60 °C to remove moisture. Then, the dry weight (W_{dry}) and length (L_{dry}) of membranes were measured. SPEEK/AGO membranes were next immersed in water at room temperature until the absorbed water saturated [18]. Finally, the wet weight (W_{wet}) and length (L_{wet}) of membranes were recorded and averaged. The water uptake (WU) and swelling degree (SD) about the SPEEK/AGO membrane were obtained by follows:

$$WU = \frac{W_{wet} - W_{dry}}{W_{dry}} \times 100\% \quad (1)$$

$$SD = \frac{L_{wet} - L_{dry}}{L_{dry}} \times 100\% \quad (2)$$

4-8. Elemental Analysis

The content of nitrogen and carbon in the SPEEK/AGO membranes was tested by elemental analyzers (Flash Smart) at room temperature.

4-9. Proton Conductivity

The proton conductivity of SPEEK/AGO membranes was tested by electrochemical work station (CHI660E, Shanghai Chenhua). The impedance value of membranes was tested by an alternating impedance spectrum. Before testing, the SPEEK/AGO membranes were immersed in water to achieve the water-absorbent balance [13]. The sample membranes were tested in the laboratory-made mold, and the transverse resistance R of the membranes was tested under RH=100%. The test method was three-probe AC impedance method, the test disturbance voltage was 5 mV, and the impedance spectrum test frequency ranged from 10^{-2} to 10^{6} Hz at 60, 80, 100 and 120 °C. Three samples of each SPEEK/X-AGO membrane were tested and averaged. Proton conductivity of the SPEEK/X-AGO membranes was calculated by applying equation:

$$\sigma = \frac{d}{RS} \quad (3)$$

where σ (mS/cm) is the proton conductivity of the test membrane, d (cm) is the thickness of the test membrane, S (cm^2) is the contact area of the electrode, R (Ω) is the resistance of the membrane.

RESULTS AND DISCUSSION

1. Characterization of GO and AGO

The peak distribution of the various chemical structures of GO and AGO was tested by FT-IR spectra and the results are illustrated in Fig. 2. Four characteristic absorption peaks at 3,425 cm^{-1}, 1,736 cm^{-1}, 1,628 cm^{-1} and 1,386 cm^{-1} are shown in the infrared spectrum of GO, which corresponds to vibrations of -OH stretching vibration, C=O stretching vibration, ether/epoxy tensile vibration, and C-O deformation [9]. New characteristic absorption peaks

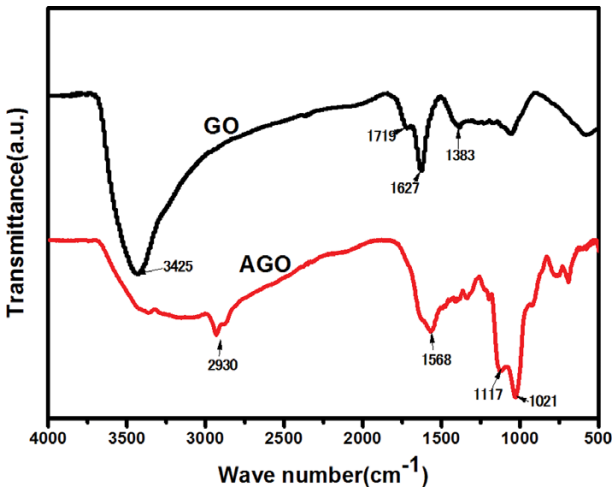

Fig. 2. FT-IR spectra of GO, AGO.

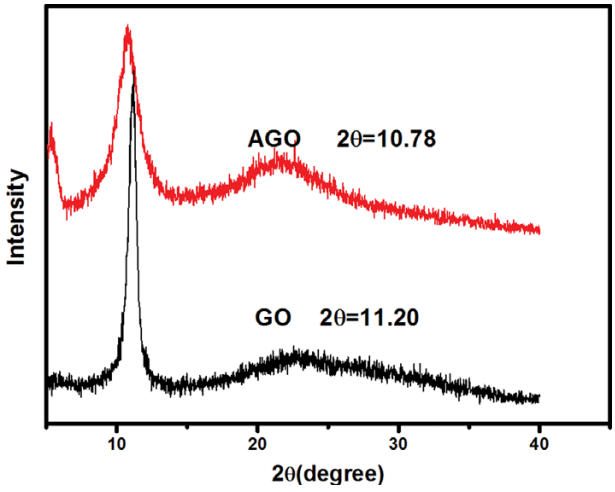

Fig. 3. XRD patterns of the GO, AGO.

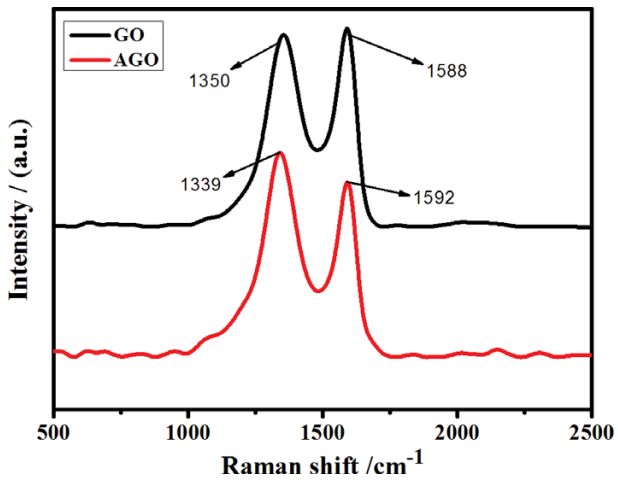

Fig. 4. Raman spectra of the GO, AGO.

appeared at 2,930 cm^{-1}, 1,568 cm^{-1}, 1,117 cm^{-1} and 1,021 cm^{-1} in that of AGO, which correspond to vibrations of -CH_2 stretching vibration, the stretching vibration of -NH_2, Si-C and Si-O-Si [13]. This indicates that the GO has been successfully grafted by APTES.

The nanocrystal structure of GO and AGO was further studied by XRD spectroscopy and illustrated in Fig. 3. GO exhibits a characteristic peak at 2θ=11.20°, and an average interlayer distance corresponding to 0.77 nm is obtained by calculation [9]. It is clearly shown that the AGO has a characteristic peak at 2θ=10.78°, which corresponds to an inter-layer distance about 0.82 nm [14]. The enlarged inter-layer distance further proves that APTES was successfully grafted onto the GO. In addition, a new weak broad diffraction peak was observed near the diffraction angle of 2θ=22.64°, caused by the functionalization of the main oxygen-containing functional group of GO. It was found that peak intensity of AGO was lower than that of the GO, and the grafting of the amorphous coupling agent gave rise to the decreasing crystallinity of GO nanoparticles [19].

The microstructure of the GO, AGO was analyzed by Raman spectroscopy, as illustrated in Fig. 4. The absorption peaks at about 1,350 cm^{-1} and 1,588 cm^{-1} correspond to the GO sheet defect peak (D peak) and the crystal carbon absorption peak (G peak) [25]. The peak of AGO appears at about 1,339 cm^{-1} (D peak) and 1,592 cm^{-1} (G peak). The peak intensity (I_D/I_G ratio) can characterize the extent of AGO defects. The I_D/I_G ratio increases from 0.97 in GO to 1.18 in AGO, which indicates that more defects are formed in AGO.

The SEM images of GO and AGO are shown in Fig. 5. It can be seen that both GO and AGO are non-smooth, pleated sheet structures, probably due to strong forces between nanoparticles. With the addition of APTES, the SEM image of AGO shows that the surface folds reduced, indicating that the force was weakened, thus reducing nanoparticle agglomeration.

2. Characterization of SPEEK/AGO Membranes

The surface and cross-section of pristine SPEEK membrane, SPEEK/2-AGO, and SPEEK/5-AGO membrane were examined by SEM. It is apparent, seen from Fig. 6, the surface and cross-section of the pristine SPEEK membrane are smooth and flat. There are no pores and obvious structural defects. The SPEEK/2-AGO composite membrane exhibited a small amount of roughness, but no obvious cracks and pores. It is demonstrated that the interaction between the sulfonic acid groups in the SPEEK and the amine group in AGO has a great effect on the uniformity of the AGO nanoparticles within the membrane. However, as the amount of AGO doping increases, the roughness of the SPEEK/AGO membrane also increases. When the amount of AGO in membranes reaches 5 wt%, the roughness increases and the surface of the composite membrane shows obvious wrinkles. The cross-section becomes rough and defects appear, showing some small pores. This is due to the dispersion of AGO in the SPEEK membrane deteriorates when the AGO content is more than 2 wt%.

Thermal performance is important for PEMFC and guarantees a long life. Fig. 7 shows the mass loss of the SPEEK/AGO membranes. As shown, all composite membranes show similar TGA curves, and the thermal loss of the SPEEK/AGO membrane can be roughly divided into three main stages [13]. The first stage of loss is at about 80 °C, which is caused by evaporation of solvent and moisture remaining in the membrane [15]. The second mass loss is at 300 °C caused by the disintegration of sulfonic acid groups of the SPEEK/AGO composite membrane [22]. The third mass loss is

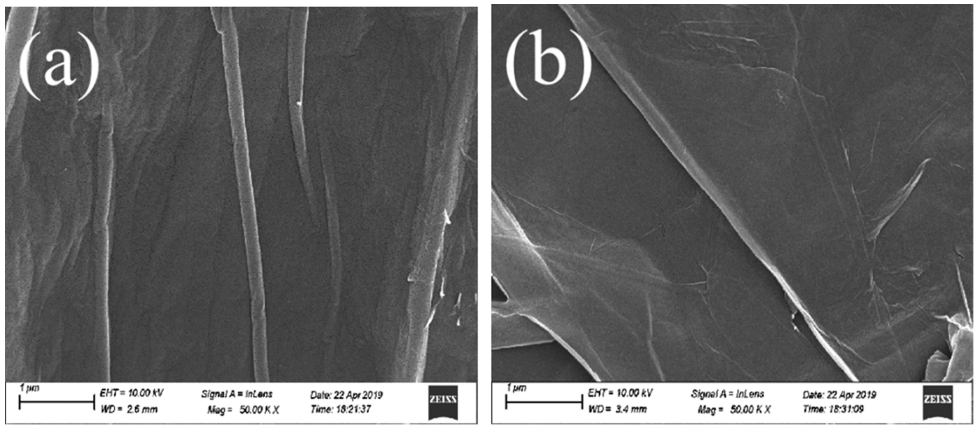

Fig. 5. SEM images of (a) GO, (b) AGO.

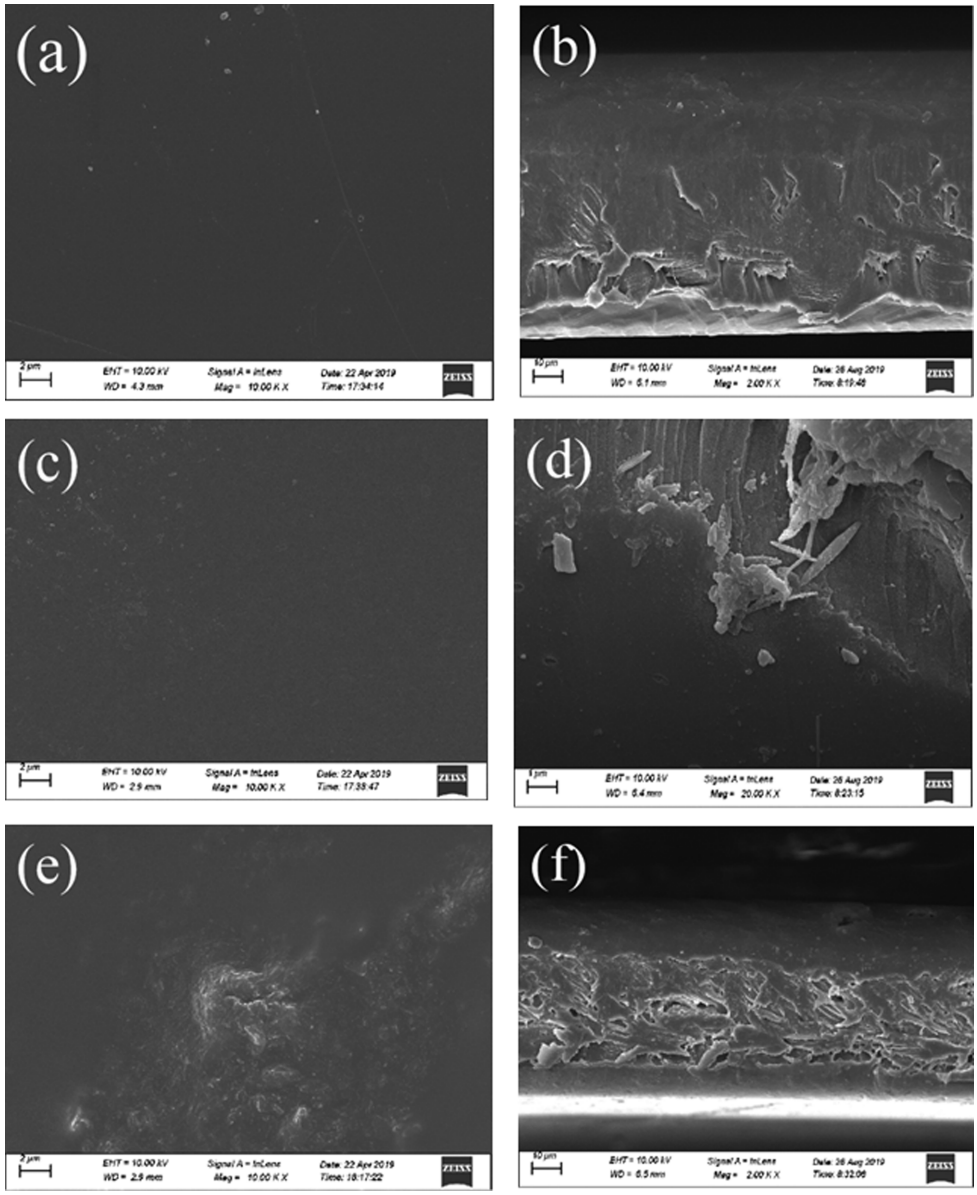

Fig. 6. SEM images of SPEEK (a) (b), SPEEK/2-AGO (c) (d) and SPEEK/5-AGO (e) (f).

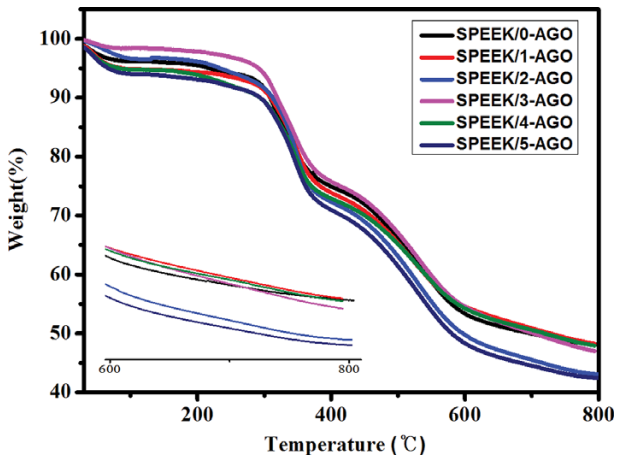

Fig. 7. TGA curves of SPEEK/X-AGO nanocomposite membranes.

attributed to the breakdown of the SPEEK polymer backbone, which occurs at approximately 450 °C [17]. The polymer membranes all show good thermal stability and satisfy the requirement of high temperature PEMFCs.

Fig. 8 summarizes the mechanical properties of the prepared SPEEK/AGO membranes. It is observed that the SPEEK/AGO composite membranes have a higher tensile strength than the pristine SPEEK membrane, indicating that the interaction between AGO and SPEEK polymer makes the membrane structure tighter, which leads to an increase in tensile strength [15]. However, the SPEEK/AGO composite membranes have a lower break elongation in comparison with the pristine SPEEK membrane, because of the formation of hydrogen bonding between nanoparticles and SPEEK membrane, which reduces the flexibility of polymer chains [50]. Therefore, the SPEEK/AGO composite membranes have distinguished mechanical properties than the pristine SPEEK mem-

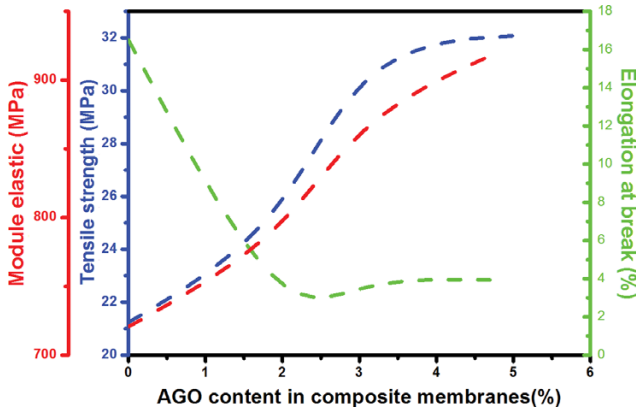

Fig. 8. The mechanical properties of SPEEK/X-AGO nanocomposite membranes.

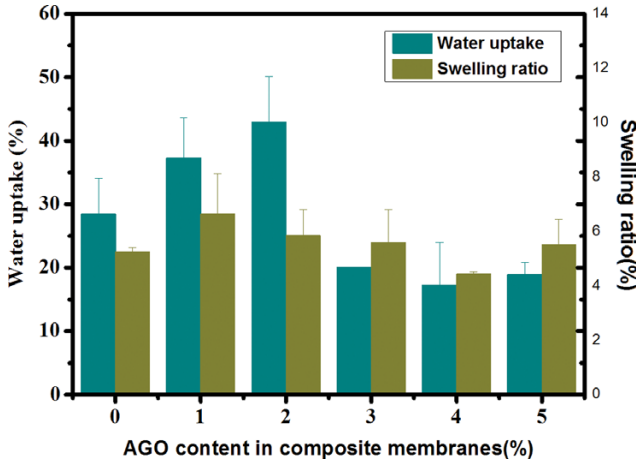

Fig. 9. Water uptake and swelling degree of the SPEEK/X-AGO membrane.

brane. The reason is that the addition of AGO improves the adhesion between SPEEK and AGO, which enhances the mechanical properties of the composite membrane.

The membrane swelling and water absorption are vital parameters for the dimensional stability of the PEM. The water uptake plays a crucial role in the proton transport, and it is closely related to the proton conductivity of the PEM. Generally, the proton conductivity of the PEM increased with the increasing of the water uptake, which is more conducive to the operation of PEMFC under higher temperature conditions [42]. Fig. 9 shows the water uptake and swelling degree of the SPEEK membrane with AGO content 0%, 1%, 2%, 3%, 4% and 5%. As the content of AGO increases, the water uptake of the membrane shows a trend of increasing first and then decreasing, as shown in Fig. 9. The water uptake reaches the maximum at 2 wt% AGO content, which is due to the formation of hydrogen bonds between the surface hydroxyl groups of AGO and free water, increasing the water retention of the composite membrane [56]. However, when the AGO content is more than 2 wt%, the water uptake shows a decreasing tendency, which is mainly attributed to the nanoparticle aggregation and blocking effects. The membranes with a high swelling degree will result in

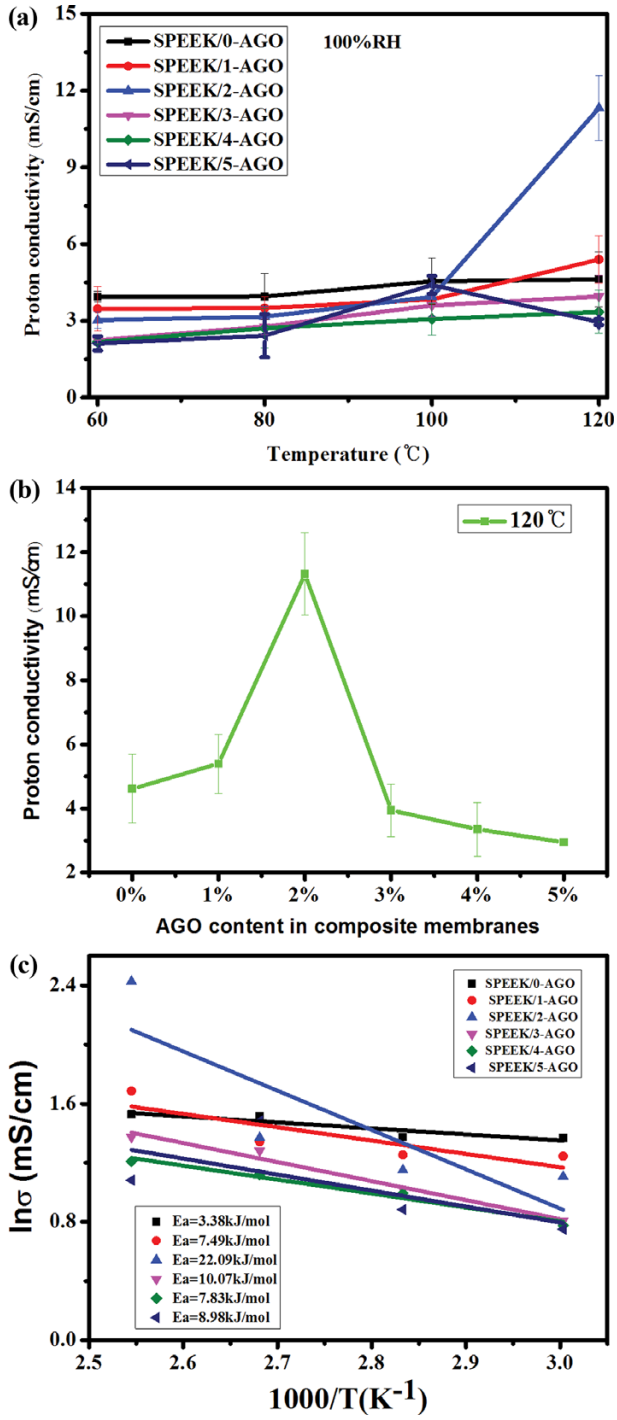

Fig. 10. (a) Proton conductivity of SPEEK membranes with different content of AGO at 60, 80, 100 and 120 °C; (b) Proton conductivity of SPEEK membranes with different content of AGO at 120 °C; (c) Arrhenius plots of proton conductivity of SPEEK membranes with different content of AGO.

poor dimensional stability and low durability, resulting in reduced fuel cell performance [19]. So, it can be obviously seen that the SPEEK/AGO membrane has a higher swelling degree in comparison with the pristine SPEEK membrane due to the water uptake increasing. However, the SPEEK/2-AGO membrane shows the high-

Table 1. Comparison of the proton conductivity of SPEEK/X-AGO membranes with other nanocomposite membranes in literature

Membrane	Filler loading (%)	Temperature (°C)	Proton conductivity (mS/cm^{-1})	Ref.
SPEEK	0	120	4.617	[This work]
SPEEK/2-AGO	2	120	11.315	[This work]
Nafion/Fe_3O_4-SGO	3	120	11.62	[3]
F-GO/Nafion	10	120	47	[4]
Nafion	—	120	12	[4]
SPES/SPB-FGO	2	25	28.9	[13]
SPEEK–DGO	7.5	120	3.26	[51]
SPEEK/PVA@GO	—	130	8.3	[57]

est water uptake but the lower swelling degree in comparison with SPEEK/1-AGO. The swelling degree of the SPEEK/AGO membrane decreases with the increase of AGO content. It is possible because AGO nanoparticles interact with the SPEEK matrix via a hydrogen bond, thereby limiting the movement of the polymer chain and controlling the swelling degree of the composite membrane.

Proton conductivity, which is one of the most crucial factors of PEM, is susceptible to many factors, such as water uptake and dispersion of inorganic fillers. Proton transport relies on two different mechanisms: vehicle mechanism and Grotthus mechanism [12]. The structure of the pristine SPEEK membrane includes the hydrocarbon backbone and the sulfonic acid group. The backbone is hydrophobic and interlaces to form an ion channel, while the sulfonic acid group is hydrophilic, allowing protons to pass through the vehicle and Grotthus mechanism in the membrane. As for the SPEEK/AGO composite membrane, hydrogen bonding is formed between AGO and free water molecules within the membrane, which promotes proton transfer. Moreover, H_3O^+ formed between proton and free water molecules within the membrane, protons transfer in the SPEEK/AGO membrane also follows the vehicle and Grotthus mechanism. The proton conductivity of SPEEK/AGO membranes at different temperature is shown in Fig. 10(a). It can be seen that the proton conductivity increases with increasing temperature and performs best at 120 °C. Fig. 10(b) displays the proton conductivity of SPEEK/AGO membranes at 120 °C. As shown, the SPEEK/2-AGO membrane had a conductivity of 11.32 mS/cm, which is about 2.45-times higher than that of the pristine SPEEK membrane. Combined with the previous results, the highest proton conductivity of the SPEEK/2-AGO composite membrane is due to its maximum water uptake. This is because the AGO nanoparticles dispersed better in the SPEEK/AGO membrane and combined with water molecules in the polymer membrane to promote the proton transfer. However, as the content of AGO continues increases, the proton conductivity begins to decline, because the accumulation of AGO acts as a barrier to the proton transfer. Therefore, the optimum content of AGO in the SPEEK/AGO membrane is 2 wt%. Fig. 10(c) shows a linear relationship between Log proton conductivity and 1,000/T. The activation energy value (E_a) was calculated using the Arrhenius equation:

$$\ln\sigma = \ln\sigma 0 - \frac{E_a}{RT} \quad (4)$$

where E_a is $-b\times R$, b the slope of the linear fit, R is the gas constant (8.314 J/mol/K). With the content of AGO within the composite membrane increasing from 0% to 5%, the activation energy showed a trend of increasing first and then decreasing, and both were lower than those of reported membranes [19,20]. For Grotthuss mechanism, the activation energy (E_a) is between 9.65 and 38.59 kJ/mol [3]. According to the result, the vehicle mechanism preferred in SPEEK and most of SPEEK/AGO composite membranes, while the Grotthuss mechanism played the dominant role in the SPEEK/2-AGO membrane.

Table 2. The content of nitrogen and carbon in the SPEEK/AGO membranes

Sample name	N (%)	C (%)
SPEEK/1-AGO	2.855	55.303
SPEEK/2-AGO	3.501	56.426
SPEEK/5-AGO	3.526	57.184

As shown in Table 1, the comparison of the proton conductivity of SPEEK/X-AGO membranes with other nanocomposite membranes in literature has been listed. SPEEK/2-AGO membrane shows better proton conductivity, indicating that this prepared membrane is suitable for use in the high temperature PEMFC.

The content of nitrogen and carbon in the SPEEK/AGO membranes is shown in Table 2. The nitrogen content of the SPEEK/1-AGO, SPEEK/2-AGO and SPEEK/5-AGO nanocomposite membranes is 2.855%, 3.501% and 3.526%. The carbon content is 55.303%, 56.426% and 57.184%. The number of -NH_2 was calculated according to reference [52] and the result means that 42 mg (2.625 mmol) -NH_2 is placed on 1 g GO. It is shown that the amino group of aminated GO has an effect on the proton conductivity of the SPEEK. Proton conductivity increased with an increasing in the AGO content, but after exceeding the optimum amount, the accumulation of filler acts as a barrier to the proton transfer.

CONCLUSIONS

SPEEK membranes incorporated with AGO were prepared by solution casting to improve the membrane proton conductivity. The results of FT-IR, XRD and Raman indicated that APTES was successfully grafted onto GO nanoparticles. The effects of AGO nanoparticles on thermal stability, mechanical property, water uptake, membrane swelling and proton conductivity of SPEEK/AGO membranes were investigated. The results show that when APTES is

grafted onto GO, the dispersion stability within SPEEK and compatibility between GO and SPEEK can be improved, which reduces the AGO aggregation. The SPEEK/AGO composite membrane has better water uptake and distinguished proton conductivity. The proton conductivity of SPEEK/2-AGO membrane reached 11.32 mS/cm at 120 °C. Moreover, the SPEEK/AGO nanocomposite membranes show better tensile strength than that of the pristine SPEEK membrane. For the next work, we will try every means to test the performance of the PEMFC with prepared SPEEK/AGO membranes. The contributions of this paper can be summarized as follows: Inexpensive SPEEK/AGO membrane with better proton conductivity and water uptake at high temperature, makes it an attractive candidate for the Nafion membrane for the high temperature PEMFC.

ACKNOWLEDGEMENT

This work was financially supported by the National Natural Science Foundation of China (No. 21306095).

REFERENCES

1. B. L. Yi, *Battery Industry*, **8**, 16 (2003).
2. D. M. Xing, X. Z. Du and J. R. Yu, *Power Technol.*, **25**, 171 (2001).
3. M. Vinothkannan, A. R. Kim and G. G. Kumar, *RSC Adv.*, **8**, 7494 (2018).
4. H. Zarrin, D. Higgins and J. Yu, *Am. Chem. Soc.*, **115**, 20774 (2011).
5. B. Zhang, Y. Cao and S. Jiang, *J. Membr. Sci.*, **518**, 243 (2016).
6. R. Kumar, C. Xu and K. Scott, *RSC Adv.*, **2**(23), 8777 (2012).
7. J. S. Kang, L. J. Ghil and Y. S. Kim, *Colloids Surf., A Physicochem. Eng. Aspects*, **313**, 207 (2008).
8. S. T. Gao, H. L. Xu and F. Zhou, *Electrochim. Acta*, **283**, 428 (2018).
9. Y. He, C. Tong and L. Geng, *J. Membr. Sci.*, **458**(10), 36 (2014).
10. C. Liu, Q. Sun and Y. Gao, *Electrochim. Acta*, **158**, 24 (2015).
11. R. P. Pandey, A. K. Thakur and V. K. Shahi, *ACS Appl. Mater. Interfaces*, **6**(19), 16993(2014).
12. R. M. Chen, F. Z. Xu and K. Fu, *Mater. Res. Bull.*, **103**, 142 (2018).
13. Y. X. Zhao, Y. Q. Fu and Y. He, *RSC Adv.*, **5**(113), 10 (2015).
14. S. Miao, H. Zhang and X. Li, *Int. J. Hydrogen Energy*, **41**(1), 331 (2015).
15. Y. Zhao, Y. Fu and B. Hu, *Solid State Ionics*, **294**, 43 (2016).
16. S. Miao, H. Zhang and X. Li, *Int. J. Hydrogen Energy*, **41**(1), 331 (2015).
17. Y. Y. Sun, S. G. Qu and J. L. Li, *Chem. Ind. Eng. Progress*, **35**(09), 2850 (2016).
18. P. Salarizadeh, M. Javanbakht and S. Pourmahdian, *RSC Adv.*, **7**(14), 8303 (2017).
19. P. Salarizadeh, M. Javanbakht and S. Pourmahdian, *Chem. Eng. J.*, **299**, 320 (2016).
20. P. Salarizadeh, M. Javanbakht and S. Pourmahdian, *Solid State Ionics*, **281**, 12 (2015).
21. Z. Liu, X. Duan and G. Qian, *Nanotechnology*, **24**(4), 045609 (2013).
22. S. T. Gao, H. L. Xu and F. Zhou, *Electrochim. Acta*, **283**, 428 (2018).
23. Y. Jiang, J. Hao and M. Hou, *Sustainable Energy Fuels*, **10**, 1039 (2017).
24. Y. Xue, R. Fu and C. Wu, *J. Membr. Sci.*, **350**(1-2), 148 (2010).
25. A. K. Mishra, N. H. Kim and D. Jung, *J. Membr. Sci.*, **458**, 128 (2014).
26. T. Jiang, T. Kuila and N. H. Kim, *Compos. Sci. Technol.*, **79**(5), 115 (2013).
27. K. Feng, B. Tang and P. Wu, *J. Mater. Chem. A*, **2**(38), 16083 (2014).
28. P. Salarizadeh, S. A. H. Maryam and A. Bagheri, *Electrochim. Acta*, **295**, 875 (2019).
29. P. Salarizadeh, M. Javanbakht and S. Pourmahdian, *J. Colloid Interface Sci.*, **472**, 135 (2016).
30. B. Mecheri, A. D'Epifanio and E. Traversa, *J. Power Sources*, **178**(2), 554 (2008).
31. C. H. Rhee, H. K. Kim and H. Chang, *Chem. Mater.*, **17**(7), 1691 (2005).
32. P. Salarizadeh, A. Bagheri and H. Beydaghi, *Int. J. Energy Res.*, **43**(9), 4840 (2019).
33. P. Salarizadeh, M. Javanbakht and S. Pourmahdian, *Int. J. Hydrogen Energy*, **44**, 3099 (2019).
34. K. Feng, B. Tang and P. Wu, *ACS Appl. Mater. Interfaces*, **5**(4), 1481 (2013).
35. R. P. Pandey, G. Shukla and M. Manohar, *Adv. Colloid Interface Sci.*, **240**, 15 (2017).
36. D. C. Marcano, D. V. Kosynkin and J. M. Berlin, *ACS Nano.*, **4**(8), 4806 (2010).
37. K. Guan, F. Liang and H. Zhu, *ACS Appl. Mater. Interfaces*, **10**, 13903 (2018).
38. T. Rattana, S. Chaiyakun and N. Witit-anun, *Procedia Eng.*, 32(7), 759 (2012).
39. W. Dai, Y. Shen and Z. Li, *J. Mater. Chem. A*, **2**(31), 12423 (2014).
40. U. R. Farooqui, A. L. Ahmad and N. A. Hamid, *Renew. Sust. Energy Rev.*, **82**, 714 (2018).
41. G. Shukla and V. K. Shahi, *Desalination*, **451**, 200 (2019).
42. Z. Jiang, X. Zhao and A. Manthiram, *Int. J. Hydrogen Energy*, **38**(14), 5875 (2013).
43. R. Kumar, M. Mamlouk and K. Scott, *RCS Adv.*, **4**(2), 617 (2013).
44. R. P. Pandey and V. K. Shahi, *J. Power Sources*, **299**, 104 (2015).
45. M. B. Askari, A. Beheshti-Marnani and M. Seifi, *J. Colloid Interface Sci.*, **537**, 186 (2019).
46. Z. Jiang, Y. Shi and Z. J. Jiang, *J. Mater. Chem. A*, **2**(18), 6494 (2014).
47. C. Lee, X. Wei and J. W. Kysar, *Science*, **321**(5887), 385 (2008).
48. A. A. Balandin, S. Ghosh and W. Bao, *Nano Lett.*, **8**(3), 902 (2008).
49. S. Hu, M. Lozada-Hidalgo and F. C. Wang, *Nature*, **516**(7530), 227 (2014).
50. J. Wang, X. Jin and C. Li, *Chem. Eng. J.*, **370**, 831 (2019).
51. Y. He, J. Wang and H. Zhang, *J. Mater. Chem. A*, **2**(25), 9548 (2014).
52. S. J. Chiong, P. S. Goh and A. F. Ismail, *J. Natural Gas Sci. Eng.*, **42**, 190 (2017).
53. F. Mengna, H. Yumin and W. Miaoqing, *Int. J. Hydrogen Energy*, **43**(24), 11214 (2018).
54. W. Rehman, K. Liaqat and S. Fazil, *J. Polymer Res.*, **26**, 3 (2019).
55. S. G. Qu, M. H. Li and C. C. Zhang, *Polymers*, **11**(1), 1 (2019).
56. H. Beydaghi and M. Javanbakht, *Ind. Eng. Chem. Res.*, **54**(28), 7028 (2015).
57. J. L. Reyes-Rodriguez, J. Escorihuela and A. García-Bernabé, *RSC Adv.*, **7**(84), 53481 (2017).